

\tilde{X}^3B_1 , \tilde{a}^1A_1 , \tilde{b}^1B_1 , and $\tilde{c}^1\Sigma_g^+$ Electronic States of NH_2^+ Jeffrey C. Stephens, Yukio Yamaguchi, C. David Sherrill,[†] and Henry F. Schaefer III*

Center for Computational Quantum Chemistry, University of Georgia, Athens, Georgia 30602-2556

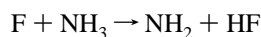
Received: January 14, 1998

Ab initio molecular electronic structure theory has been employed in order to investigate systematically the \tilde{X}^3B_1 , \tilde{a}^1A_1 , \tilde{b}^1B_1 , and $\tilde{c}^1\Sigma_g^+$ states of NH_2^+ , with emphasis placed on the \tilde{b}^1B_1 and $\tilde{c}^1\Sigma_g^+$ states. The self-consistent-field (SCF), configuration interaction with single and double excitations (CISD), complete active space (CAS) SCF, and CASSCF second-order configuration interaction (SOC) wave functions with nine basis sets, the largest being a triple- ζ basis set with three sets of polarization functions and two additional sets of higher angular momentum and diffuse functions [TZ3P(2f,2d)+2diff], were used to determine equilibrium geometries, harmonic vibrational frequencies, infrared (IR) intensities, and dipole moments. The ground, first, and second excited states are confirmed to be bent, while the third excited state is predicted to be linear. The bond angles of NH_2^+ are shown to be larger than those of the corresponding isoelectronic CH_2 molecule. At the highest level of theory, TZ3P(2f,2d)+2diff CASSCF-SOCI, the triplet–singlet splitting is predicted to be 29.4 kcal/mol (1.28 eV, 10 300 cm^{-1}), which is in good agreement with the experimental observation of 30.1 kcal/mol (1.305 eV, 10 530 cm^{-1}). With the same method, the second excited state (\tilde{b}^1B_1) lies 43.7 kcal/mol (1.89 eV, 15 300 cm^{-1}) above the ground state, which is significantly lower than the experimentally proposed value of 2.54 eV. The third excited state ($\tilde{c}^1\Sigma_g^+$) is predicted to lie 77.0 kcal/mol (3.34 eV, 26 900 cm^{-1}) above the ground state. The equilibrium geometry of this $\tilde{c}^1\Sigma_g^+$ state is determined to be $r_e = 1.030$ Å at the TCSCF-CISD level with the largest basis set. Since the IR intensities of all active vibrational modes are predicted to be substantial, IR spectroscopic studies of the four states are feasible. However, of the six fundamentals experimentally assigned to date, two appear to be incorrect. The energy separations among the four lowest-lying states of NH_2^+ are found to be larger than the corresponding states of CH_2 .

I. Introduction

The nitrenium ion (NH_2^+) is worthy of study because of its similarities and differences to the well-studied isoelectronic methylene (CH_2) molecule and its relevance to organic chemistry with properties associated to both carbenes and carbonium molecules. As the simplest nitrenium whose excited states have been implicated in stereoselective organic chemistry, understanding of this model system may lead to insights into some of its peculiar chemistry.

The first experimental work on the nitrenium ion was carried out by Dunlavey, Dyke, Jonathan, and Morris in 1980.¹ They recorded the HeI photoelectron spectrum of the NH_2 (\tilde{X}^2B_1) radical produced from the rapid reaction



Three bands were observed corresponding to ionization of NH_2 (\tilde{X}^2B_1) to the \tilde{X}^3B_1 , \tilde{a}^1A_1 , and \tilde{b}^1B_1 states of NH_2^+ . They determined the triplet–singlet splitting to be 0.99 ± 0.02 eV from measurement of the first two adiabatic ionization potentials (11.46 and 12.45 eV) of NH_2 . Dunlavey also detected a band assigned to the ionization process $NH_2^+ (^1B_1) \leftarrow NH_2 (\tilde{X}^2B_1)$ at 13.68 eV (adiabatic) and 14.27 eV (vertical). They were able to determine the vibrational frequencies for the ground and first two excited states. The Southampton group measured an 840

± 50 cm^{-1} bending frequency for the 3B_1 ground state, 2900 ± 50 cm^{-1} symmetric stretch, and 1350 ± 50 cm^{-1} bending motion, for the 1A_1 state, and a 920 ± 150 cm^{-1} bending motion for the 1B_1 state. These researchers used ab initio self-consistent-field (SCF) and configuration interaction (CI) methods with a Gaussian basis set of double- ζ plus polarization quality to characterize their photoelectron spectra.

Gibson, Greene, and Berkowitz reported the photoionization mass spectrum of NH_2 , prepared by the reaction $H + N_2 H_4$.² They determined the adiabatic ionization potential of NH_2 to be 11.14 ± 0.01 eV (0.032 eV lower than the previous PES value¹). They also observed a prominent autoionizing Rydberg series, converging to the excited \tilde{a}^1A_1 state at 12.445 ± 0.002 eV. Thus, their adiabatic energy gap between \tilde{X}^3B_1 and the lowest singlet (\tilde{a}^1A_1) state is 1.305 ± 0.01 eV $\equiv 30.1 \pm 0.2$ kcal/mol.

Jensen, Bunker, and McLean calculated the rotation–vibration energies of singlet and triplet NH_2^+ using the Morse oscillator–rigid bender internal dynamics (MORBID) Hamiltonian in 1987.³ Ab initio points on the potential energy surfaces were determined employing a multiconfiguration (MC) self-consistent-field (SCF) second-order configuration interaction (SOC) method with a contracted Gaussian basis of size N (4s3p2p1f) and H (3s2p). Their best estimates for the fundamental vibrational frequencies of the \tilde{X}^3B_1 state are $\nu_1 = 3118$, $\nu_2 = 918$, and $\nu_3 = 3363$ cm^{-1} , while those of the \tilde{a}^1A_1 state are $\nu_1 = 3027$, $\nu_2 = 1289$, and $\nu_3 = 3111$ cm^{-1} .

[†] Present address: Department of Chemistry, University of California, Berkeley, CA 94720.

In 1989, Okumura, Rehffuss, Dinelli, Bawendi, and Oka used difference frequency laser absorption spectroscopy to measure the asymmetric stretching frequency (ν_3) for the \tilde{X}^3B_1 state of NH_2^+ .⁴ They observed the ν_3 fundamental band in the infrared using velocity modulated detection of the ions created in an ac discharge. The origin of the ν_3 band was found to be $\nu_0 = 3359.932\text{ cm}^{-1}$. This is reasonably close to the ab initio prediction of a scaled SCF harmonic frequency of 3308 cm^{-1} by DeFrees and McLean.⁵ Their results are in excellent agreement with the fundamental value of 3363 cm^{-1} theoretically predicted by Jensen, Bunker, and McLean.³

The most recent experimental study on NH_2^+ was carried out by Kabbadj, Huet, Uy, and Oka in 1996.⁶ They recorded the absorption spectrum of NH_2^+ continuously between 3500 and 2900 cm^{-1} with a difference frequency laser spectrometer along with a velocity modulated technique and observed four new hot bands of the NH_2^+ ion in the region of the ν_3 fundamental band. In view of the very low barrier to linearity and the high bending vibrational states involved, the authors analyzed the observed spectrum using the Hamiltonian for linear molecules. The equilibrium rotational constant was determined to be $B_e = 8.022\,966\text{ cm}^{-1}$, which gives the equilibrium bond length $r_e = 1.021\text{ \AA}$. They also estimated the ν_2 bending vibrational frequency to be around 439 cm^{-1} from the value of the l -type doubling constant.

The very first ab initio theoretical study of NH_2^+ was performed by Peyerimhoff, Buenker, and Allen⁷ in 1966 as one of seven polyhydrides (four of the type AH_2 and three of the type AH_3) in conjunction with the empirical orbital binding energy diagrams of Walsh.⁸ Using the SCF method and Gaussian lobe functions as a basis, set they computed a series of single point energies to determine the equilibrium bond angle of the closed-shell 1A_1 state of NH_2^+ . At a fixed bond distance of 2.05 au , they found the minimum energy bond angle to be 120° .

In 1971, Chu, Siu, and Hayes calculated the four lowest electronic states of NH_2^+ with a double- ζ basis set (DZ) and truncated configuration interaction (CI) methods.⁹ They determined the 3B_1 configuration to be the ground state with a bond angle of 130° . The lowest 1A_1 state was calculated to be 1.56 eV above the ground state with a bond angle of 120° . The other excited states were found to lie above the ground state by 2.03 and 3.30 eV for the 1B_1 and second 1A_1 states, respectively. They also reported a barrier to linearity for the ground state to be 320 cm^{-1} . In the same year, Lee and Morokuma investigated the singlet–triplet splitting of NH_2^+ using a DZ CI method.¹⁰ The almost linear 3B_1 ground state was found to lie below the 1A_1 state by 1.95 eV with the bond angle of 115° .

Further theoretical work by Harrison and Eakers in 1973 found different geometries for the two lowest states with a DZ CI level of theory.¹¹ They found an r_e bond length of 1.906 au and an angle of 120° for the 1A_1 state. They also stated that the lowest 1A_1 state lies above the 150° 3B_1 ground state by 1.95 eV . Bender, Meadows, and one of us reported in 1977 the singlet–triplet separation of NH_2^+ to be 29.1 kcal/mol at the SCF/TCSCF level of theory with a near Hartree–Fock limit basis set.¹² In that study, also presented were equilibrium geometries for these two lowest states of NH_2^+ .

In 1979, Peyerimhoff and Buenker reported multireference configuration interaction (MRD-CI) calculations for the lowest 14 states of the NH_2^+ ion using 52 contracted Gaussian functions as a basis set.¹³ They obtained angular and NH symmetric stretch curves and considered distortions involving

asymmetric conformations. They determined the bond angles (in degrees) and relative energies at a fixed NH distance of $1.940\,775\text{ au}$:

$$^3B_1 < ^1A_1 < ^1B_1 < 2^1A_1$$

$$0.0 < 1.29\text{ eV} < 2.03\text{ eV} < 3.45\text{ eV}$$

$$150 < 108 < 155 < 180$$

They also determined the barrier to linearity for the ground state to be 330 cm^{-1} , in close agreement with prior theoretical studies.⁹

Chambaud, Gabriel, Schmelz, Rosmus, Spielfiedel, and Feautrier computed the rotational–vibrational spectra of the three lowest states of NH_2^+ in 1993 with complete active space computations (CASSCF) and multireference configuration interaction out of the CASSCF orbitals giving the CASSCF-MRCI method.¹⁴ Combined with Dunning's correlation consistent quadruple- ζ basis set, they mapped out the potential energy surfaces of these lowest states and determined anharmonic frequencies, barriers to linearity, energy differences between the states, and geometric parameters.

In 1993, Barclay, Hamilton, and Jensen calculated the 30 lowest vibrational energy levels for the \tilde{X}^3B_1 and \tilde{a}^1A_1 states of CH_2 and NH_2^+ for various potential energy surfaces and reported a new surface for the NH_2^+ triplet state, with predicted fundamentals $\nu_1 = 3059$, $\nu_2 = 845$, and $\nu_3 = 3360\text{ cm}^{-1}$.¹⁵ Their bending frequency of 845 cm^{-1} is in good agreement with the experimental estimate at $840 \pm 50\text{ cm}^{-1}$ determined by Dunlavey and co-workers¹ and asymmetric stretching frequency of 3360 cm^{-1} in excellent agreement with the experimental value of 3359.9 cm^{-1} by Okumura et al.⁴

In recent work we reported systematic characterizations of the four lowest-lying states of isoelectronic CH_2 ^{16–19} and isovalent SiH_2 ²⁰ and PH_2^+ .²¹ In the present study the four electronically low-lying states of NH_2^+ are investigated by using SCF, two-configuration (TC)SCF, CASSCF,^{22–24} SCF-(TCSCF)-CISD, and CASSCF second-order configuration interaction (SOC) wave functions with nine different basis sets. Special emphasis is placed on the second (\tilde{b}^1B_1) and third ($\tilde{c}^1\Sigma_g^+$) excited states in order to encourage further experimental characterization of these states.

II. Electronic Structure Considerations

The lowest state of linear NH_2^+ has the following electronic configuration:

$$(1\sigma_g)^2(2\sigma_g)^2(1\sigma_u)^2(1\pi_u)^2$$

This degenerate π^2 configuration gives rise to three electronic states, $^3\Sigma_g^+$, $^1\Delta_g$, and $^1\Sigma_g^+$. As NH_2^+ deviates from $D_{\infty h}$ symmetry (linear) to a C_{2v} symmetry (bent), the $^3\Sigma_g^+$ state transforms as 3B_1 giving the electronic configuration

$$^3\Sigma_g^+ \rightarrow (1a_1)^2(2a_1)^2(1b_2)^2(3a_1)^1(1b_1)^1 \quad \tilde{X}^3B_1$$

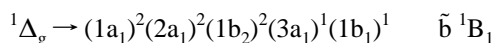
The $^1\Delta_g$ state undergoes Renner–Teller splitting to form two states favorable to bending with electronic configurations of

$$^1\Delta_g \rightarrow (1a_1)^2(2a_1)^2(1b_2)^2(3a_1)^2 \quad \tilde{a}^1A_1 (1^1A_1)$$

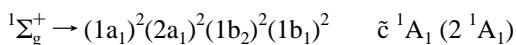
and

TABLE 1: Theoretical Predictions of the Total Energy (in hartree), Bond Length (in Å), Bond Angle (in deg), Dipole Moment (in D), Harmonic Vibrational Frequencies (in cm⁻¹), Infrared Intensities (in Parentheses in km mol⁻¹), and Zero-Point Vibrational Energy (ZPVE in kcal mol⁻¹) for the Bent \tilde{X}^3B_1 Ground State of the NH₂⁺ Molecule

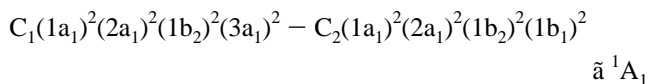
level of theory	energy	r_e	θ_e	μ_e	$\omega_1(a_1)$	$\omega_2(a_1)$	$\omega_3(b_2)$	ZPVE
DZP SCF	-55.219 778	1.0230	143.08	0.877	3478(71.4)	1098(124.5)	3721(613.3)	11.86
TZ2P SCF	-55.227 492	1.0173	142.85	0.846	3453(56.5)	1113(120.5)	3693(565.7)	11.81
TZ2P+diff SCF	-55.227 505	1.0173	142.83	0.846	3453(56.4)	1113(120.0)	3693(566.5)	11.81
TZ3P SCF	-55.227 432	1.0181	142.92	0.841	3435(54.9)	1110(120.3)	3676(567.8)	11.75
TZ3P+2diff SCF	-55.227 462	1.0181	142.93	0.841	3435(55.1)	1109(120.1)	3676(568.1)	11.75
TZ2P(f,d) SCF	-55.228 153	1.0181	143.01	0.844	3443(57.0)	1108(121.6)	3684(571.9)	11.77
TZ2P(f,d)+diff SCF	-55.228 175	1.0181	142.99	0.844	3443(56.6)	1109(121.3)	3684(571.9)	11.77
TZ3P(2f,2d) SCF	-55.228 361	1.0179	142.98	0.839	3439(55.2)	1110(120.4)	3681(568.5)	11.77
TZ3P(2f,2d)+2diff SCF	-55.228 409	1.0179	142.98	0.839	3439(55.1)	1110(120.3)	3682(568.1)	11.77
DZP CISD	-55.344 601	1.0381	149.14	0.786	3329(47.9)	840(143.2)	3573(602.3)	11.07
TZ2P CISD	-55.368 678	1.0281	150.08	0.725	3300(36.5)	831(140.6)	3547(586.4)	10.98
TZ2P+diff CISD	-55.368 837	1.0281	150.02	0.726	3301(36.6)	834(140.1)	3547(586.1)	10.98
TZ3P CISD	-55.369 771	1.0295	149.97	0.722	3277(35.4)	831(138.4)	3523(588.4)	10.91
TZ3P+2diff CISD	-55.370 009	1.0295	149.96	0.723	3277(35.6)	831(138.3)	3523(588.3)	10.91
TZ2P(f,d) CISD	-55.382 687	1.0295	150.88	0.712	3296(35.8)	797(145.2)	3545(610.0)	10.92
TZ2P(f,d)+diff CISD	-55.382 719	1.0295	150.85	0.712	3295(35.5)	798(144.8)	3545(609.9)	10.92
TZ3P(2f,2d) CISD	-55.387 403	1.0281	150.40	0.714	3295(35.6)	814(141.5)	3549(602.8)	10.95
TZ3P(2f,2d)+2diff CISD	-55.387 464	1.0281	150.40	0.715	3295(35.5)	814(141.4)	3549(602.4)	10.95
exptl (ref 6)		1.021				439		
exptl (ref 1)						840 ± 50		
exptl (ref 4)							3359.9	



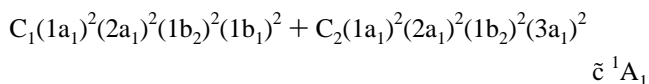
with the \tilde{b}^1B_1 state being an open-shell singlet. The ${}^1\Sigma_g^+$ state transforms as 1A_1 giving an electronic configuration of



The \tilde{a}^1A_1 state is represented by a two-configurational wave function to account for the excitations of electrons from the $3a_1$ to $1b_1$ orbitals as bending occurs. Thus, the electronic configuration for the \tilde{a}^1A_1 state was defined as



Moreover, the $\tilde{c}^1\Sigma_g^+$ state requires a multireference method since it shares the same symmetry as a lower state; thus its electronic configuration is represented as a double excitation from the \tilde{a}^1A_1 state giving



For both bent 1A_1 states, the C_1 component is greater than the C_2 component. In the case of linear $\tilde{c}^1\Sigma_g^+$, the C_1 and C_2 coefficients must be equal since the $3a_1$ and $1b_1$ orbitals become degenerate.

III. Theoretical Procedures

Nine different basis sets were chosen in this research. A Huzinaga double- ζ (9s5p) primitive basis set²⁶ contracted to (4s2p) by Dunning²⁷ was augmented by one set of polarization functions on both the hydrogen ($\alpha_p = 0.75$) and the nitrogen ($\alpha_d = 0.80$) to give a DZP basis set with a contraction scheme of (9s5p1d)/(4s2p1d) for nitrogen and (4s1p)/(2s1p) for hydrogen.

A Dunning²⁸ contracted Huzinaga triple- ζ basis set²⁶ was used for the rest of the study. This (10s6p) primitive set was contracted to (5s3p) for nitrogen and a (5s) primitive basis set to (3s) for hydrogen. This TZ basis set was first augmented

with two sets of polarization functions [$\alpha_d(N) = 1.60, 0.40$; $\alpha_p(H) = 1.50, 0.375$] giving a TZ2P basis set. Then the nitrogen was augmented with a diffuse s ($\alpha_s = 0.067 42$) function and a set of diffuse p ($\alpha_p = 0.049 59$) functions, while the hydrogen was augmented with a diffuse s ($\alpha_s = 0.030 16$) function giving a TZ2P+diff basis set. The TZ2P was further expanded by the addition of one set of higher angular momentum functions giving a TZ2P(f,d) where the nitrogen has a set of f functions ($\alpha_f = 1.0$) and the hydrogen a set of d functions ($\alpha_d = 1.0$). The TZ2P(f,d)+diff basis set was obtained using the diffuse functions from the TZ2P+diff and the higher angular momentum functions in the TZ2P(f,d) set.

The TZ basis set was also augmented by three sets of polarization functions giving the TZ3P set. This included three sets of d functions on nitrogen, $\alpha_d = 3.2, 0.8, 0.2$, and three sets of p functions on hydrogen, $\alpha_p = 3.0, 0.75, 0.1875$. This basis set was further increased by the addition of two sets of diffuse functions (TZ3P+2diff) with nitrogen ($\alpha_s = 0.067 42, 0.023 00$; $\alpha_p = 0.049 59, 0.018 09$) and hydrogen ($\alpha_s = 0.030 16, 0.009 247$). The last two basis sets are a TZ3P augmented with two sets of higher angular momentum functions; two sets of f functions on nitrogen ($\alpha_f = 2.0, 0.50$) and two sets of d functions for hydrogen ($\alpha_d = 2.0, 0.50$) giving the TZ3P(2f,2d) basis set and the TZ3P(2f,2d)+2diff set with the two sets of diffuse functions taken from above. The largest basis set, TZ3P(2f,2d) + 2diff, comprises 112 contracted Gaussian functions with a contraction scheme of N (12s8p3d2f/7s5p3d2f) and H (7s3p2d/5s3p2d).

Equilibrium geometries, harmonic vibrational frequencies, dipole moments, and infrared (IR) intensities were determined at the self-consistent-field (SCF) and configuration interaction with single and double excitations (CISD) levels of theory. For the \tilde{X}^3B_1 and \tilde{b}^1B_1 states, a single reference SCF wave function was used while a two-configuration (TC) SCF reference wave function was used for the \tilde{a}^1A_1 and $\tilde{c}^1\Sigma_g^+$ states. Moreover, complete active space (CAS) SCF methods were applied. The CAS space included all six valence electrons in the six valence molecular orbitals. Furthermore, configuration interaction wave functions with all single and double excitations out of the references generated by the CASSCF were constructed (CASSCF-SOCI) to determine more reliable relative energetics.

TABLE 2: Theoretical Predictions of the Total Energy (in hartree), Bond Length (in Å), Bond Angle (in deg), Dipole Moment (in D), Harmonic Vibrational Frequencies (in cm⁻¹), Infrared Intensities (in Parentheses in km mol⁻¹), and Zero-Point Vibrational Energy (ZPVE in kcal mol⁻¹) for the Bent \tilde{a}^1A_1 State of the NH₂⁺ Molecule

level of theory	energy	r_e	θ_e	μ_e	$\omega_1(a_1)$	$\omega_2(a_1)$	$\omega_3(b_2)$	ZPVE
DZP TCSCF	-55.170 652	1.0348	108.37	2.246	3468(82.4)	1546(103.4)	3554(231.9)	12.25
TZ2P TCSCF	-55.180 608	1.0312	108.22	2.142	3428(66.1)	1564(109.2)	3498(216.7)	12.14
TZ2P+diff TCSCF	-55.180 652	1.0313	108.21	2.140	3428(65.8)	1564(108.7)	3498(217.2)	12.14
TZ3P SCF	-55.180 809	1.0319	108.07	2.125	3413(63.7)	1564(110.1)	3485(218.1)	12.10
TZ3P+2diff TCSCF	-55.180 837	1.0319	108.07	2.125	3413(63.7)	1564(109.6)	3485(217.8)	12.10
TZ2P(f,d) TCSCF	-55.181 886	1.0316	108.56	2.137	3420(67.1)	1546(108.3)	3494(221.4)	12.09
TZ2P(f,d)+diff TCSCF	-55.181 916	1.0316	108.55	2.136	3420(66.8)	1545(107.7)	3493(221.2)	12.09
TZ3P(2f,2d) TCSCF	-55.182 494	1.0315	108.54	2.120	3417(63.4)	1544(108.7)	3491(222.0)	12.08
TZ3P(2f,2d)+2diff TCSCF	-55.182 527	1.0315	108.54	2.120	3417(63.2)	1544(108.3)	3491(221.5)	12.08
DZP TCSCF-CISD	-55.294 761	1.0523	107.15	2.228	3283(55.7)	1443(88.0)	3382(163.5)	11.59
TZ2P TCSCF-CISD	-55.320 133	1.0446	107.51	2.126	3234(49.4)	1453(98.0)	3313(173.5)	11.44
TZ2P+diff TCSCF-CISD	-55.320 290	1.0446	107.50	2.125	3233(49.1)	1452(97.4)	3312(174.0)	11.43
TZ3P TCSCF-CISD	-55.321 532	1.0465	107.49	2.103	3212(46.3)	1450(99.7)	3295(176.7)	11.37
TZ3P+2diff TCSCF-CISD	-55.321 785	1.0465	107.50	2.103	3212(46.3)	1450(99.2)	3295(176.6)	11.38
TZ2P(f,d) TCSCF-CISD	-55.336 021	1.0459	107.96	2.131	3233(53.2)	1424(100.5)	3318(186.1)	11.40
TZ2P(f,d)+diff TCSCF-CISD	-55.336 067	1.0460	107.94	2.131	3233(53.1)	1423(99.8)	3317(186.1)	11.40
TZ3P(2f,2d) TCSCF-CISD	-55.341 612	1.0445	107.99	2.110	3239(50.1)	1429(102.5)	3324(189.7)	11.42
TZ3P(2f,2d)+2diff TCSCF-CISD	-55.341 668	1.0445	107.99	2.110	3239(50.0)	1429(102.1)	3324(189.2)	11.42
exptl (ref 1)					2900 ± 50	1350 ± 50		

TABLE 3: Theoretical Predictions of the Total Energy (in hartree), Bond Length (in Å), Bond Angle (in deg), Dipole Moment (in D), Harmonic Vibrational Frequencies (cm⁻¹), Infrared Intensities (in Parentheses in km mol⁻¹), and Zero-Point Vibrational Energy (ZPVE in kcal mol⁻¹) for the Bent \tilde{b}^1B_1 State of the NH₂⁺ Molecule

level of theory	energy	r_e	θ_e	μ_e	$\omega_1(a_1)$	$\omega_2(a_1)$	$\omega_3(b_2)$	ZPVE
DZP SCF	-55.143 116	1.0246	160.69	0.580	3439(27.2)	607(241.2)	3720(869.9)	11.10
TZ2P SCF	-55.150 718	1.0186	158.37	0.599	3413(23.5)	692(207.6)	3690(788.6)	11.14
TZ2P+diff SCF	-55.150 723	1.0186	158.35	0.599	3413(23.7)	692(207.0)	3690(787.7)	11.14
TZ3P SCF	-55.150 700	1.0192	158.45	0.590	3399(22.5)	689(204.0)	3677(786.2)	11.10
TZ3P+2diff SCF	-55.150 740	1.0192	158.44	0.592	3399(22.8)	691(204.3)	3676(785.7)	11.10
TZ2P(f,d) SCF	-55.153 922	1.0192	160.23	0.555	3405(20.2)	632(217.2)	3688(808.7)	11.04
TZ2P(f,d)+diff SCF	-55.153 930	1.0192	160.20	0.556	3405(20.2)	633(216.6)	3688(808.2)	11.04
TZ3P(2f,2d) SCF	-55.154 477	1.0189	160.30	0.549	3401(19.1)	631(214.0)	3685(801.9)	11.03
TZ3P(2f,2d)+2diff SCF	-55.154 517	1.0189	160.30	0.549	3401(19.1)	630(214.3)	3686(801.4)	11.03
DZP CISD	-55.268 091	1.0386	157.12	0.697	3314(31.5)	664(230.4)	3582(748.6)	10.81
TZ2P CISD	-55.294 503	1.0285	157.58	0.632	3282(22.4)	676(208.7)	3550(712.9)	10.73
TZ2P+diff CISD	-55.294 661	1.0285	157.44	0.635	3282(22.8)	682(207.8)	3550(710.7)	10.74
TZ3P CISD	-55.295 775	1.0298	157.55	0.623	3263(21.4)	667(202.7)	3530(711.8)	10.66
TZ3P+2diff CISD	-55.296 029	1.0298	157.50	0.626	3262(21.8)	669(202.9)	3529(710.8)	10.66
TZ2P(f,d) CISD	-55.312 536	1.0293	161.47	0.531	3284(16.1)	542(224.4)	3562(760.0)	10.56
TZ2P(f,d)+diff CISD	-55.312 560	1.0293	161.41	0.533	3284(16.1)	544(223.8)	3562(759.2)	10.56
TZ3P(2f,2d) CISD	-55.318 182	1.0280	160.96	0.538	3280(16.1)	562(217.2)	3562(748.2)	10.59
TZ3P(2f,2d)+2diff CISD	-55.318 233	1.0280	160.92	0.539	3281(16.1)	564(217.5)	3562(747.5)	10.59
exptl (ref 1)						920 ± 150		

In all of the CISD and SOCI procedures, one core (N 1s-like) orbital was frozen and the corresponding virtual (N 1s*-like) orbital was deleted. With the largest basis set, TZ3P(2f, 2d)+2diff, the numbers of configuration state functions (CSFs) for the CISD wave functions in C_{2v} symmetry are 19 628 (\tilde{X}^3B_1 , SCF reference), 26 658 (\tilde{a}^1A_1 , TCSCF reference), 19 554 (\tilde{b}^1B_1 , SCF reference), and 26 658 ($\tilde{c}^1\Sigma_g^+$, TCSCF reference), respectively. The numbers of the CSFs for the CASSCF wave functions are 51 (\tilde{X}^3B_1), 56 (\tilde{a}^1A_1), 39 (\tilde{b}^1B_1), and 56 ($\tilde{c}^1\Sigma_g^+$), respectively. With the largest basis set the numbers of CSFs in C_{2v} symmetry for the CASSCF-SOCI wave functions are 446 330 (\tilde{X}^3B_1), 296 371 (\tilde{a}^1A_1), 283 116 (\tilde{b}^1B_1), and 296 371 ($\tilde{c}^1\Sigma_g^+$), respectively.

Gradients from the SCF and CISD methods were obtained analytically, whereas the TCSCF-CISD gradients for the $\tilde{c}^1\Sigma_g^+$ state were evaluated via finite differences of energies. Dipole moments with respect to the center of mass were computed as explicit energy derivatives in terms of an electric field; however, for the $\tilde{c}^1\Sigma_g^+$ state at the TCSCF-CISD level of theory, they were obtained as expectation values. Harmonic vibrational frequencies at the SCF and TCSCF level were

determined analytically, while at the CISD and TCSCF-CISD levels of theory they were evaluated by finite differences of analytic gradients. The TCSCF-CISD vibrational frequencies for the $\tilde{c}^1\Sigma_g^+$ state were computed via numerical differentiation of energies. The electronic energy of the $\tilde{c}^1\Sigma_g^+$ state was obtained from the second root of the TCSCF, CISD, and SOCI Hamiltonians, respectively. The total energy of the (TC)SCF, CISD, CASSCF, and SOCI wave functions were converged to 10^{-12} hartrees, and geometric parameters were optimized to 10^{-6} atomic units. All computations were carried out using the Psi 2.0.8 program package.²⁹

IV. Results and Discussion

Table 1 contains SCF and CISD energies, equilibrium bond lengths, bond angles, dipole moments, and harmonic vibrational frequencies with IR intensities, and zero-point vibrational energies (ZPVEs) for the \tilde{X}^3B_1 state at the 18 levels of theory. In Tables 2 and 3, the corresponding quantities for the \tilde{a}^1A_1 state and \tilde{b}^1B_1 state are provided. The comparable quantities for the $\tilde{c}^1\Sigma_g^+$ state from TCSCF reference wave functions are presented in Table 4. Table 5 contains the CASSCF and

TABLE 4: Theoretical Predictions of the Total Energy (in hartree), Bond Length (in Å), Bond Angle (in deg), Dipole Moment (in D), Harmonic Vibrational Frequencies (in cm⁻¹), Infrared Intensities (in Parentheses in km mol⁻¹), and Zero-Point Vibrational Energy (ZPVE in kcal mol⁻¹) for the Linear (Bent) $\tilde{c}^1\Sigma_g^+$ (2^1A_1) State of the NH₂⁺ Molecule

level of theory	energy	r_e	θ_e	μ_e	$\omega_1(\sigma_g, a_1)$	$\omega_2(\pi, a_1)$	$\omega_3(\sigma_u, b_2)$	ZPVE
DZP TCSCF	-55.072 920	1.0253	180.0	0.0	3435(0.0)	556(737.2)	3727(1007.7)	11.83
TZ2P TCSCF	-55.080 252	1.0189	180.0	0.0	3403(0.0)	515(624.8)	3696(931.6)	11.62
TZ2P+diff TCSCF	-55.080 255	1.0189	180.0	0.0	3403(0.0)	514(621.0)	3696(931.5)	11.62
TZ3P SCF	-55.080 286	1.0192	180.0	0.0	3397(0.0)	525(599.7)	3689(923.8)	11.63
TZ3P+2diff TCSCF	-55.080 315	1.0192	180.0	0.0	3396(0.0)	521(605.1)	3689(923.3)	11.62
TZ2P(f,d) TCSCF	-55.081 883	1.0199	180.0	0.0	3396(0.0)	552(624.5)	3693(936.1)	11.71
TZ2P(f,d)+diff TCSCF	-55.081 886	1.0199	180.0	0.0	3396(0.0)	551(624.1)	3693(936.5)	11.71
TZ3P(2f,2d) TCSCF	-55.082 147	1.0195	180.0	0.0	3391(0.0)	552(606.1)	3691(921.1)	11.70
TZ3P(2f,2d)+2diff TCSCF	-55.082 179	1.0195	180.0	0.0	3392(0.0)	552(606.9)	3691(921.0)	11.70
DZP TCSCF-CISD	-55.213 010	1.0396	178.03	0.072	3305(0.3)	125(385.6)	3587(950.1)	10.03
TZ2P TCSCF-CISD	55.239 603	1.0299	176.17	0.126	3261(0.7)	249(314.3)	3541(878.2)	10.08
TZ2P+diff TCSCF-CISD	-55.239 754	1.0300	175.68	0.141	3260(0.9)	282(309.9)	3540(877.3)	10.13
TZ3P TCSCF-CISD	-55.241 005	1.0309	178.27	0.055	3255(0.1)	110(304.9)	3532(871.6)	9.86
TZ3P+2diff TCSCF-CISD	-55.241 264	1.0309	178.15	0.060	3255(0.2)	117(307.9)	3533(870.9)	9.87
TZ2P(f,d) TCSCF-CISD	-55.257 330	1.0315	180.0	0.0	3263(0.0)	289(648.2)	3553(896.6)	10.57
TZ2P(f,d)+diff TCSCF-CISD	-55.257 355	1.0314	180.0	0.0	3262(0.0)	285(648.4)	3552(897.2)	10.56
TZ3P(2f,2d) TCSCF-CISD	-55.262 826	1.0299	180.0	0.0	3260(0.0)	254(623.9)	3551(878.4)	10.46
TZ3P(2f,2d)+2diff TCSCF-CISD	-55.262 871	1.0299	180.0	0.0	3260(0.0)	253(625.1)	3551(878.4)	10.46

TABLE 5: Total CASSCF and CASSCF SOCI Energies in hartrees at the CISD Optimized Geometries for Several Electronic States of the NH₂⁺ Molecule

level of theory	state, reference wave function			
	\tilde{X}^3B_1 , SCF	\tilde{a}^1A_1 , TCSCF	\tilde{b}^1B_1 , SCF	$\tilde{c}^1\Sigma_g^+$, TCSCF
DZP CASSCF	-55.266 985	-55.216 423	-55.178 347	-55.128 375
TZ2P CASSCF	-55.274 954	-55.228 232	-55.187 088	-55.136 315
TZ2P+diff CASSCF	-55.274 974	-55.228 282	-55.187 124	-55.136 325
TZ3P CASSCF	-55.275 029	-55.228 450	-55.187 177	-55.136 373
TZ3P+2diff CASSCF	-55.275 078	-55.228 486	-55.187 243	-55.136 420
TZ2P(f,d) CASSCF	-55.275 655	-55.229 539	-55.189 852	-55.138 039
TZ2P(f,d)+diff CASSCF	-55.275 676	-55.229 574	-55.189 873	-55.138 043
TZ3P(2f,2d) CASSCF	-55.275 999	-55.230 203	-55.190 701	-55.138 313
TZ3P(2f,2d)+2diff CASSCF	-55.276 048	-55.230 237	-55.190 750	-55.138 348
DZP CASSCF SOCI	-55.348 716	-55.298 720	-55.271 478	-55.218 271
TZ2P CASSCF SOCI	-55.373 814	-55.325 018	-55.298 890	-55.246 046
TZ2P+diff CASSCF SOCI	-55.373 976	-55.325 180	-55.299 054	-55.246 203
TZ3P CASSCF SOCI	-55.374 942	-55.326 448	-55.300 184	-55.247 496
TZ3P+2diff CASSCF SOCI	-55.375 189	-55.326 713	-55.300 445	-55.247 763
TZ2P(f,d) CASSCF SOCI	-55.388 368	-55.341 292	-55.317 269	-55.264 168
TZ2P(f,d)+diff CASSCF SOCI	-55.388 400	-55.341 340	-55.317 293	-55.264 195
TZ3P(2f,2d) CASSCF SOCI	-55.393 210	-55.347 039	-55.323 037	-55.269 815
TZ3P(2f,2d)+2diff CASSCF SOCI	-55.393 270	-55.347 097	-55.323 089	-55.269 860

CASSCF-SOCI energies for all four states at the CISD optimized geometries with the same basis set. Table 6 has the relative energies of the three excited states with respect to the ground state both with and without ZPVE correction.

A. Geometries. At the TZ3P(2f,2d)+2diff CISD level of theory, the equilibrium bond lengths (in Å) of the four lowest states of NH₂⁺ are in the order

$$\tilde{a}^1A_1 (1.045) > \tilde{c}^1\Sigma_g^+ (1.030) > \tilde{X}^3B_1 (1.0281) > \tilde{b}^1B_1 \quad (1.0280)$$

while the ordering of the corresponding four states of CH₂¹⁶ is

$$\tilde{a}^1A_1 (1.105) > \tilde{X}^3B_1 (1.075) > \tilde{b}^1B_1 (1.071) > \tilde{c}^1A_1 \quad (1.064)$$

The $\tilde{c}^1\Sigma_g^+$ state of NH₂⁺ has a longer bond length (1.030 Å) than the \tilde{X}^3B_1 state (1.0281 Å), although the \tilde{X}^3B_1 state of CH₂ has a longer bond length (1.075 Å) than the \tilde{c}^1A_1 state (1.064 Å). It is seen that the NH bond lengths are significantly shorter than the CH bond lengths, probably owing to the larger electronegativity of the N atom. With the same method, the

equilibrium bond angles (in degrees) of the four states of NH₂⁺ are in the order

$$\tilde{c}^1\Sigma_g^+ (180.0) > \tilde{b}^1B_1 (160.9) > \tilde{X}^3B_1 (150.4) > \tilde{a}^1A_1 \quad (108.0)$$

which is consistent with the ordering of the corresponding four states of CH₂¹⁶

$$\tilde{c}^1A_1 (171.6) > \tilde{b}^1B_1 (142.9) > \tilde{X}^3B_1 (132.9) > \tilde{a}^1A_1 \quad (102.3)$$

It is observed, however, that the bond angle of each state of NH₂⁺ is considerably larger than that of the corresponding state of CH₂.

The present theoretically predicted structure of the ground state ($r_e = 1.0281$ Å and $\theta_e = 150.40^\circ$) may be compared with the geometry ($r_e = 1.0338$ Å and $\theta_e = 153.17^\circ$) via the MCSCF-SOCI method by Jensen et al.³ and that ($r_e = 1.0294$ Å and $\theta_e = 152.07^\circ$) via the CASSCF-MRCI by Chambaud et al.¹⁴ The experimental bond length of the ground state of NH₂⁺ is determined to be $r_e = 1.021$ Å, assuming a linear structure,⁶ which is 0.007 Å shorter than our theoretical value mentioned

TABLE 6: Relative Energies T_e in kcal mol⁻¹ (T_0 Value in Parentheses) for Several Electronic States of the NH₂⁺ Molecule^a

level of theory	state, reference wave function			
	\tilde{X}^3B_1 , SCF	\tilde{a}^1A_1 , TCSCF	\tilde{b}^1B_1 , SCF	$\tilde{c}^1\Sigma_g^+$, TCSCF
DZP (TC)SCF	0.0	30.83(31.22)	48.11(47.35)	92.15(92.12)
TZ2P (TC)SCF	0.0	29.42(29.75)	48.18(47.51)	92.39(92.20)
TZ2P+diff (TC)SCF	0.0	29.40(29.73)	48.18(47.51)	92.40(92.21)
TZ3P (TC)SCF	0.0	29.26(29.61)	48.15(47.50)	92.34(92.22)
TZ3P+2diff (TC)SCF	0.0	29.26(29.61)	48.14(47.49)	92.34(92.21)
TZ2P(f,d) (TC)SCF	0.0	29.03(29.35)	46.58(45.85)	91.79(91.73)
TZ2P(f,d)+diff (TC)SCF	0.0	29.03(29.35)	46.59(45.86)	91.80(91.74)
TZ3P(2f,2d) (TC)SCF	0.0	28.78(29.09)	46.36(45.62)	91.75(91.68)
TZ3P(2f,2d)+2diff (TC)SCF	0.0	28.79(29.10)	46.37(45.63)	91.76(91.69)
DZP CASSCF	0.0	31.73(32.25)	55.62(55.36)	86.98(85.94)
TZ2P CASSCF	0.0	29.32(29.78)	55.14(54.89)	87.00(86.10)
TZ2P+diff CASSCF	0.0	29.30(29.75)	55.13(54.89)	87.00(86.15)
TZ3P CASSCF	0.0	29.23(29.69)	55.13(54.88)	87.01(85.96)
TZ3P+2diff CASSCF	0.0	29.24(29.71)	55.12(54.87)	87.01(85.97)
TZ2P(f,d) CASSCF	0.0	28.94(29.42)	53.84(53.48)	86.36(86.01)
TZ2P(f,d)+diff CASSCF	0.0	28.93(29.41)	53.84(53.48)	86.37(86.01)
TZ3P(2f,2d) CASSCF	0.0	28.74(29.21)	53.53(53.17)	86.40(85.91)
TZ3P(2f,2d)+2diff CASSCF	0.0	28.75(29.22)	53.53(53.17)	86.41(85.92)
DZP CISD	0.0	31.28(31.80)	48.01(47.75)	82.57(81.53)
TZ2P CISD	0.0	30.46(30.92)	46.55(46.30)	81.00(80.10)
TZ2P+diff CISD	0.0	30.46(30.91)	46.55(46.31)	81.00(80.15)
TZ3P CISD	0.0	30.27(30.73)	46.43(46.18)	80.80(79.75)
TZ3P+2diff CISD	0.0	30.26(30.73)	46.42(46.17)	80.79(79.75)
TZ2P(f,d) CISD	0.0	29.28(29.76)	44.02(43.66)	78.66(78.31)
TZ2P(f,d)+diff CISD	0.0	29.27(29.75)	44.03(43.67)	78.67(78.31)
TZ3P(2f,2d) CISD	0.0	28.73(29.20)	43.44(43.08)	78.17(77.68)
TZ3P(2f,2d)+2diff CISD	0.0	28.74(29.21)	43.44(43.08)	78.18(77.69)
DZP CASSCF SOCI	0.0	31.37(31.89)	48.47(48.21)	81.86(80.82)
TZ2P CASSCF SOCI	0.0	30.62(31.08)	47.02(46.77)	80.18(79.28)
TZ2P+diff CASSCF SOCI	0.0	30.62(31.07)	47.01(46.77)	80.18(79.33)
TZ3P CASSCF SOCI	0.0	30.43(30.89)	46.91(46.66)	79.97(78.92)
TZ3P+2diff CASSCF SOCI	0.0	30.42(30.89)	46.90(46.65)	79.96(78.92)
TZ2P(f,d) CASSCF SOCI	0.0	29.54(30.02)	44.62(44.26)	77.94(77.59)
TZ2P(f,d)+diff CASSCF SOCI	0.0	29.53(30.01)	44.62(44.26)	77.94(77.58)
TZ3P(2f,2d) CASSCF SOCI	0.0	28.97(29.44)	44.03(43.67)	77.43(76.94)
TZ3P(2f,2d)+2diff CASSCF SOCI	0.0	28.97(29.44)	44.04(43.68)	77.44(76.95)
exptl (ref 2)	0.0	(30.1)		

^a Note that the CISD results for the \tilde{a}^1A_1 and $\tilde{c}^1\Sigma_g^+$ states are actually two reference CISD results. A single reference CISD approach would be less than satisfactory for these two electronic states.

above. The NH bond lengths of the four states are always predicted to be longer at the CISD level than the SCF method, as is usually the case.³⁰⁻³³

The bond angle of the \tilde{X}^3B_1 state increases with inclusion of correlation effects, while that of the \tilde{a}^1A_1 state decreases. The structures of the \tilde{X}^3B_1 and \tilde{b}^1B_1 states are quite similar, since they have the same electronic configuration, coupling the two open-shell electrons with different spin multiplicity. The $\tilde{c}^1\Sigma_g^+$ state is predicted to be linear with the TCSCF method. However, at the TCSCF-CISD level of theory, this state is predicted to be slightly bent using the basis sets without higher angular momentum functions, whereas it is linear when higher angular momentum functions are included. It is found that³⁴ a DZP full CI wave function provides a bent structure, while the TZ2P(f,d) CASSCF-SOCI method predicts a linear structure for the $\tilde{c}^1\Sigma_g^+$ state.

According to the Walsh diagram for an AH₂ (A being a heavy atom) type molecule,⁸ the 3a₁ orbital prefers a bent structure; however, the 1b₁ orbital favors a linear structure. Thus, a qualitative prediction for the four lowest states of NH₂⁺ is the \tilde{a}^1A_1 state with two electrons in the 3a₁ orbital is significantly bent, the \tilde{X}^3B_1 and \tilde{b}^1B_1 states with one electron in the 3a₁ orbital and one electron in the 1b₁ orbital are quasi-linear, and the $\tilde{c}^1\Sigma_g^+$ state, with two electrons in the 1b₁ orbital, is linear.

The present study as well as previous ab initio studies quantitatively support the Walsh rule.

B. Dipole Moments. At the highest CISD level of theory for which geometry optimizations were carried out, the TZ3P-(2d,2f)+2diff (TC)SCF-CISD method, the magnitudes of the predicted equilibrium dipole moments (in debye) for the four electronic states of NH₂⁺ are in the order

$$\tilde{a}^1A_1 (2.110) > \tilde{X}^3B_1 (0.715) > \tilde{b}^1B_1 (0.539) > \tilde{c}^1\Sigma_g^+ (0.0) \quad (0.0)$$

which are compared with those of the corresponding four states of CH₂¹⁶

$$\tilde{a}^1A_1 (1.690) > \tilde{b}^1B_1 (0.669) > \tilde{X}^3B_1 (0.600) > \tilde{c}^1A_1 (0.205)$$

Although the first three states of NH₂⁺ have significantly larger bond angles than those of CH₂, the dipole moments of the two molecules are comparable. The large dipole moment of the \tilde{a}^1A_1 state makes it a likely candidate for microwave spectroscopic observation. The predicted dipole moments generally decrease with inclusion of correlation effects and with expansion of basis set size.

C. Harmonic Vibrational Frequencies. With the largest (TC)SCF-CISD method the magnitude of the two stretching frequencies [$\omega_1(a_1)$ and $\omega_3(b_2)$ in cm⁻¹] are in the order

$$\tilde{X}^3B_1 (3295) > \tilde{b}^1B_1 (3281) > \tilde{c}^1\Sigma_g^+ (3260) > \tilde{a}^1A_1 \quad (3239)$$

for the $\omega_1(a_1)$ symmetric stretch mode and

$$\tilde{b}^1B_1 (3562) > \tilde{c}^1\Sigma_g^+ (3551) > \tilde{X}^3B_1 (3549) > \tilde{a}^1A_1 \quad (3324)$$

for the $\omega_3(b_2)$ antisymmetric stretch mode. The ordering of these two modes are almost consistent with Badger's rule^{35,36} that the stretching vibrational frequencies generally decrease with increase of the corresponding bond lengths. Usually the bending frequency decreases with an increase of the corresponding bond angle. The bending frequencies [$\omega_2(a_1)$ in cm⁻¹] of NH₂⁺ fall in this category: the order of the $\omega_2(a_1)$ frequencies for the four states is

$$\tilde{a}^1A_1 (1429) > \tilde{X}^3B_1 (814) > \tilde{b}^1B_1 (564) > \tilde{c}^1\Sigma_g^+ (253)$$

This ordering is consistent with that of the bending frequencies of CH₂¹⁶

$$\tilde{a}^1A_1 (1420) > \tilde{X}^3B_1 (1134) > \tilde{b}^1B_1 (967) > \tilde{c}^1A_1 (552)$$

It is clearly seen that the bending potentials of the \tilde{X}^3B_1 and \tilde{b}^1B_1 states of NH₂⁺ are significantly floppier than the corresponding states of CH₂. This feature is nicely illustrated in Figure 1 of ref 6.

The two stretching frequencies of the \tilde{X}^3B_1 state decrease with inclusion of correlation effects owing to longer bond distances. Similarly, the bending frequency of the ground state significantly decreases at the CISD level owing to larger bond angles. With the most complete CISD method, the antisymmetric stretch frequency [$\omega_3(b_2)$] is predicted to be 3549 cm⁻¹. This compares favorably to the experimental fundamental frequency of 3360 cm⁻¹ by Okumura et al.⁴ with a difference of 189 cm⁻¹, which may be largely attributed to anharmonic effects. The $\omega_2(a_1)$ mode predicted at 814 cm⁻¹ falls within the experimental error of the measured frequency of 840 ± 50 cm⁻¹ by Dunlavey and co-workers.¹

For the \tilde{a}^1A_1 state, the two stretching frequencies show similar tendencies as for the ground state. The bending frequency of this first excited state decreases with inclusion of correlation effects, although the bond angle is predicted to be smaller at the CISD level of theory. The two a_1 harmonic frequencies, 3239 (ω_1) and 1429 cm⁻¹ (ω_2), with the largest CI method, agree reasonably well with the fundamental frequencies (2900 ± 50 and 1350 ± 50 cm⁻¹) determined via PES.¹ The three vibrational frequencies of the \tilde{b}^1B_1 state decrease with improving treatment of correlation effects, as is the case for the ground state. The experimentally "measured" fundamental frequency of 920 ± 150 cm⁻¹ by Dunlavey and associates¹ appears to be much too high, considering a larger bond angle ($\sim 161^\circ$) of this second excited state than that ($\sim 150^\circ$) of the ground state.

D. Infrared (IR) Intensities. Owing to greater charge separation (A⁻H⁺), the IR intensities of NH₂⁺ are drastically larger than those of CH₂. Specifically, the IR intensities (in km/mol) of asymmetric stretching mode (ω_3) for NH₂⁺ are in

the order of

$$\tilde{c}^1\Sigma_g^+ (878) > \tilde{b}^1B_1 (748) > \tilde{X}^3B_1 (602) > \tilde{a}^1A_1 (189)$$

while those of CH₂¹⁶ are

$$\tilde{c}^1A_1 (76) > \tilde{a}^1A_1 (68) > \tilde{b}^1B_1 (15) > \tilde{X}^3B_1 (0.1)$$

Indeed Oka's research group was able to detect the ν_3 fundamental band of the ground state of NH₂⁺ via difference laser spectroscopy.^{4,6} Since all vibrational modes except the symmetric stretching mode (ω_1) of the $\tilde{c}^1\Sigma_g^+$ state provide substantial IR intensities, all four lowest-lying states of NH₂⁺ may be suitable for IR spectroscopic investigations.

E. Energetics. Using the largest basis set, the T_e and T₀ values for the first excited state (\tilde{a}^1A_1) at the four levels of theory are predicted to be 28.79 and 29.10 kcal/mol (SCF/TCSCF), 28.75 and 29.22 kcal/mol (CASSCF), 28.74 and 29.21 kcal/mol (TCSCF-CISD), and 28.97 and 29.44 kcal/mol (CASSCF-SOCI), respectively. This triplet-singlet splitting diminishes with the increase of basis set size by about 2.5 kcal/mol. Our best T₀ value, 29.4 kcal/mol (1.28 eV, 10 300 cm⁻¹), is in good agreement with the experimental value of 30.1 kcal/mol (1.305 eV, 10530 cm⁻¹) by Gibson et al.² rather than the earlier experimental T₀ value of 0.99 eV by Dunlavey et al.¹ The previous theoretical predictions, based on highly correlated levels of theory, the T_e = 29.9 kcal/mol (MRD-CI) by Peyerimhoff and Buenker,¹³ T_e = 10 475 cm⁻¹ (MCSCF-SOCI) by Jensen et al.,³ and T_e = 10 193 cm⁻¹ (CASSCF-MRCI) by Chambaud et al.¹⁴ agree quite well with our results.

The energy separation between the ground and second excited state is more sensitive to correlation effects and basis set size than the previous case. The best theoretical T₀ value for the \tilde{b}^1B_1 state in this study is 43.7 kcal/mol (1.89 eV, 15 300 cm⁻¹), which is consistent with the previous studies of T_e = 15 397 cm⁻¹ (MCSCF-SOCI) by Jensen et al.³ and T_e = 15 263 cm⁻¹ (CASSCF-MRCI) by Chambaud et al.¹⁴ The corresponding experimental T₀ value is estimated to be 58.6 kcal/mol (2.540 eV, 20 490 cm⁻¹) after correction of the first adiabatic ionization potential.^{1,2,37} Referring to the good agreement for the previous energy gap (error being only 0.7 kcal/mol), the estimated experimental T₀ value (2.540 eV) appears to be too high.

The T_e and T₀ values for the $\tilde{c}^1\Sigma_g^+$ state are even more sensitive to the level of sophistication and basis set size. The difference in the largest and smallest T values are about 15 kcal/mol. Our best T₀ value is predicted, at the CASSCF-SOCI level of theory, to be 77.0 kcal/mol (3.34 eV, 26 900 cm⁻¹).

In summary, the relative energies corrected for ZPVE (in kcal/mol) of the four lowest-lying states of the NH₂⁺ ion at the highest level of theory are

$$\tilde{X}^3B_1 (0.0) < \tilde{a}^1A_1 (29.4) < \tilde{b}^1B_1 (43.7) < \tilde{c}^1\Sigma_g^+ (77.0)$$

while those of the corresponding states of the CH₂ radical¹⁶ are

$$\tilde{X}^3B_1 (0.0) < \tilde{a}^1A_1 (9.0) < \tilde{b}^1B_1 (33.2) < \tilde{c}^1A_1 (59.1)$$

The energy separation of the four states of NH₂⁺ is considerably larger than that of CH₂.

V. Conclusions

Among the four lowest-lying states of NH₂⁺, the ground and second excited states are confirmed to be quasi-linear and the third excited state is predicted to be linear with a small bending

vibrational frequency. Theoretical prediction of the molecular geometries and physical properties for NH_2^+ are found to be quite sensitive to the level of sophistication and the basis set. At the highest level of theory, TZ2P(2f,2d)+2diff CASSCF-SOCI, the T_0 values for the first ($\tilde{a} \ ^1A_1$) and second ($\tilde{b} \ ^1B_1$) excited states are predicted to be 29.4 kcal/mol (1.28 eV, 10 300 cm^{-1}) and 43.7 kcal/mol (1.89 eV, 15 300 cm^{-1}), respectively. The third excited state ($\tilde{c} \ ^1\Sigma_g^+$) is determined to be linear with a bond length of 1.030 Å and to lie 77.0 kcal/mol (3.34 eV, 26 900 cm^{-1}) above the ground state ($\tilde{X} \ ^3B_1$). We hope this study would encourage further experimental characterization of the lower-lying states of NH_2^+ , specifically the $\tilde{b} \ ^1B_1$ and $\tilde{c} \ ^1\Sigma_g^+$ states.

Acknowledgment. We thank T. J. Van Huis and M. L. Leininger for very helpful discussions. This research was supported by the U. S. National Science Foundation, grant CHE-9527468.

References and Notes

- (1) Dunlavey, S. J.; Dyke, J. M.; Jonathan, N.; Morris, A. *Mol. Phys.* **1980**, *39*, 1121.
- (2) Gibson, S. T.; Greene, J. P.; Berkowitz, J. *J. Chem. Phys.* **1985**, *83*, 4319.
- (3) Jensen, P.; Bunker, P. R.; McLean, A. D. *Chem. Phys. Lett.* **1987**, *141*, 53.
- (4) Okumura, M.; Rehfuss, B. D.; Dinelli, B. M.; Bawendi, M. G.; Oka, T. *J. Chem. Phys.* **1989**, *90*, 5918.
- (5) DeFrees, D. J.; McLean, A. D. *J. Chem. Phys.* **1985**, *82*, 333.
- (6) Kabbadj, Y.; Huet, T. R.; Uy, D.; Oka, T. *J. Mol. Spectrosc.* **1996**, *175*, 277.
- (7) Peyerimhoff, S. D.; Buenker, R. J.; Allen, L. C. *J. Chem. Phys.* **1966**, *45*, 734.
- (8) Walsh, A. D. *J. Chem. Soc.* **1953**, 2260.
- (9) Chu, S. Y.; Siu, A. K. Q.; Hayes, E. F. *J. Am. Chem. Soc.* **1971**, *94*, 2969.
- (10) Lee, S. T.; Morokuma, K. *J. Am. Chem. Soc.* **1971**, *93*, 6863.
- (11) Harrison, J. F.; Eakers, C. W. *J. Am. Chem. Soc.* **1973**, *95*, 3467.
- (12) Bender, C. F.; Meadows, J. H.; Schaefer, H. F. *Faraday Discuss. Chem. Soc.* **1977**, *62*, 59.
- (13) Peyerimhoff, S. D.; Buenker, R. J. *Chem. Phys.* **1979**, *42*, 167.
- (14) Chambaud, G.; Gabriel, W.; Schmelz, T.; Rosmus, P.; Spielfiedel, A.; Feautrier, N. *Theor. Chim. Acta.* **1993**, *87*, 5.
- (15) Barclay, V. J.; Hamilton, I. P.; Jensen, P. *J. Chem. Phys.* **1993**, *99*, 9709.
- (16) Yamaguchi, Y.; Sherrill, C. D.; Schaefer, H. F. *J. Phys. Chem.* **1996**, *100*, 7911.
- (17) Sherrill, C. D.; Van Huis, T. J.; Yamaguchi, Y.; Schaefer, H. F. *J. Mol. Struct.: THEOCHEM* **1997**, *400*, 139.
- (18) Sherrill, C. D.; Leininger, M. L.; Van Huis, T. J.; Schaefer, H. F. *J. Chem. Phys.* **1998**, *108*, 1040.
- (19) Yamaguchi, Y.; Schaefer, H. F. *Chem. Phys.* **1977**, *225*, 23.
- (20) Yamaguchi, Y.; Van Huis, T. J.; Sherrill, C. D.; Schaefer, H. F. *Theor. Chem. Acc.* **1997**, *97*, 341.
- (21) Van Huis, T. J.; Yamaguchi, Y.; Sherrill, C. D.; Schaefer, H. F. *J. Phys. Chem.* **1997**, *101*, 6955.
- (22) Siegbahn, P. E. M.; Heiberg, A.; Roos, B. O.; Levy, B. *Phys. Scr.* **1980**, *21*, 323.
- (23) Roos, B. O.; Taylor, P. R.; Siegbahn, P. E. M. *Chem. Phys.* **1980**, *48*, 157.
- (24) Roos, B. O. *Int. J. Quantum Chem.* **1980**, *S14*, 175.
- (25) Schaefer, H. F. Ph.D. Thesis, Stanford University, Stanford, CA, 1969.
- (26) Huzinaga, S. *J. Chem. Phys.* **1965**, *42*, 1293.
- (27) Dunning, T. H. *J. Chem. Phys.* **1970**, *53*, 2823.
- (28) Dunning, T. H. *J. Chem. Phys.* **1971**, *55*, 716.
- (29) Janssen, C. L.; Seidl, E. T.; Scuseria, G. E.; Hamilton, T. P.; Yamaguchi, Y.; Remington, R. B.; Xie, Y.; Vacek, G.; Sherrill, C. D.; Crawford, T. D.; Fermann, J. T.; Allen, W. D.; Brooks, B. R.; Fitzgerald, G. B.; Fox, D. J.; Gaw, J. F.; Handy, N. C.; Laidig, W. D.; Lee, T. J.; Pitzer, R. M.; Rice, J. E.; Saxe, P.; Scheiner, A. C.; Schaefer, H. F. *PSI 2.0.8*; PSITECH, Inc.; Watkinsville, GA 30677, **1995**.
- (30) Yamaguchi, Y.; Schaefer, H. F. *J. Chem. Phys.* **1980**, *73*, 2310.
- (31) Besler, B. H.; Scuseria, G. E.; Scheiner, A. C.; Schaefer, H. F. *J. Chem. Phys.* **1988**, *89*, 360.
- (32) Thomas, J. R.; DeLeeuw, B. J.; Vacek, G.; Schaefer, H. F. *J. Chem. Phys.* **1993**, *98*, 1336.
- (33) Thomas, J. R.; DeLeeuw, B. J.; Vacek, G.; Crawford, T. D.; Yamaguchi, Y.; Schaefer, H. F. *J. Chem. Phys.* **1993**, *99*, 403.
- (34) Van Huis, T. J.; Leininger, M. L.; Sherrill, C. D.; Schaefer, H. F. To be submitted.
- (35) Badger, R. M. *J. Chem. Phys.* **1934**, *2*, 128.
- (36) Badger, R. M. *J. Chem. Phys.* **1935**, *3*, 710.
- (37) Jacox, M. E. *Vibrational and Electronic Energy Levels of Polyatomic Transient Molecules*; J. Phys. Chem. Ref. Data #3; American Institute of Physics: Woodbury, NY, 1994.